Unusually Deep Wintertime Cirrus Clouds Observed over the Alaskan Sub-Arctic

James R. Campbell[1] and David A. Peterson
Naval Research Laboratory
Monterey, California, USA

Jared W. Marquis
University of North Dakota, Department of Atmospheric Sciences
Grand Forks, North Dakota, USA

Gilberto J. Fochesatto
University of Alaska Fairbanks, Department of Atmospheric Sciences
Fairbanks, Alaska, USA

Mark A. Vaughan
NASA Langley Research Center
Hampton Roads, Virginia, USA

Sebastian A. Stewart and Jason L. Tackett
Science Systems and Applications Inc.
Greenbelt, Maryland USA

Simone Lolli
Consiglio Nazionale Delle Ricerche, Istituto di Metodologie per l'Analisi Ambientale
Potenza, Italy

Jasper R. Lewis
University of Maryland Baltimore County
Baltimore, Maryland USA

Mayra I. Oyola
American Society for Engineering Education
c/o Monterey, California, USA

Ellsworth J. Welton
NASA Goddard Space Flight Center
Greenbelt, Maryland, USA

To Be Submitted As a *[Map Room]* Article to

Bulletin of the American Meteorological Society

---

[1] *Corresponding Author Address:* c/o 7 Grace Hopper Ave. Stop 2, Monterey, CA, 93943 USA; *e-mail:*james.campbell@nrlmry.navy.mil

1 ***Background.*** Unusually deep wintertime cirrus clouds at altitudes exceeding 13.0 km

2 above mean sea level (AMSL) were observed at Fairbanks, Alaska (64.86° N, 147.85° W, 0.300

3 km AMSL) over a twelve hour period, beginning near 1200 UTC 1 January 2017. Such

4 elevated cirrus cloud heights are far more typical of warmer latitudes, and in many instances

5 associated with convective outflow, as opposed to early winter over the sub-Arctic on a day

6 featuring barely four hours of local sunlight. In any other context, they could have been

7 confused for polar stratospheric clouds, which are a more common regional/seasonal occurrence

8 at elevated heights. The mechanics of this unique event are documented, including the

9 thermodynamic and synoptic environments that nurtured and sustained cloud formation. The

10 impact of an unusually deep and broad anticyclone over the wintertime Alaskan sub-Arctic is

11 described. Comparisons with climatological datasets illustrate how unusual these events are

12 regionally and seasonally. The event proves a relatively uncharacteristic confluence of

13 circulatory and dynamic features over the wintertime Alaskan sub-Arctic. Our goal is to

14 document the occurrence of this event within the context of a growing understanding for how

15 cirrus cloud incidence and their physical characteristics vary globally.

16 Cirrus clouds are unique within the earth-atmosphere system. Formed by the freezing of

17 submicron haze particles in the upper troposphere, they are the last primary cloud mechanism

18 contributing to the large scale exchange of the terrestrial water cycle. Accordingly, cirrus clouds

19 are observed globally at all times of the year, exhibiting an instantaneous global occurrence rate

20 near 40%. Radiatively, however, they are even more distinct. During daylight hours, cirrus are

21 the only cloud genus that can induce either positive or negative top-of-the-atmosphere forcing

22 (i.e., heating or cooling; all other clouds induce a negative sunlit cooling effect). Though diffuse

23 compared with low-level liquid water clouds, their significance radiatively and thus within

24   climate, is borne out of their overwhelming relative occurrence rate. This emerging recognition

25   makes understanding cirrus cloud occurrence and physical cloud properties an innovative and

26   exciting element of current climate study. The observations described here contribute to this

27   knowledge, and the apparent potential for anomalous wintertime radiative characteristics

28   exhibited along sub-Arctic latitudes.

29

30   ***Cloud Observations.***   Shown in Fig. 1 are Level 1 normalized relative backscatter data

31   (MHz·km^2·uJ^{-1}) processed by the NASA Micro Pulse Lidar Network (MPLNET) for 1-2 January

32   2017, based on measurements collected with an eye-safe 532 nm single-channel elastic-

33   backscatter lidar run autonomously atop the Geophysical Institute building on the west end of the

34   University of Alaska Fairbanks campus. Intermittent low-level liquid water and mixed-phase

35   clouds were observed throughout the first 12 hours of 1 January. These clouds are easily

36   distinguished by their relatively low base altitudes and high levels of signal attenuation

37   beginning immediately above cloud base. Lidars, much like the human eye, cannot resolve

38   targets beyond a range-integrated optical depth approaching 3.0 (two-way path-integrated

39   transmission rates approaching as low as 0.1%), and this limits the ability of lidars to fully

40   profile such clouds containing any significant concentration of liquid water droplets. On the

41   other hand, cirrus clouds, which consist solely of ice crystals, are far more likely to be

42   transparent. Cirrus clouds are exponentially more frequent at the very lowest optical depths.

43   Diffuse cirrus clouds were apparent early on the 1st near 0300 UTC between 10.0 and 11.0 km.

44   Beginning near 1200 UTC, breaks began occurring regularly in the mixed-phase cloud deck

45   near 6.0 km (this and all subsequent heights are AMSL; note the diffuse ice virga streaks

46   emanating below cloud base in Fig. 1, which are a distinct lidar signature for mixed-phase

47   clouds). These breaks allowed for the profiling of increasingly dense cirrus fallstreaks in the

48   upper troposphere. Cloud top heights in these cirrus layers initially approached 12.0 km. By

49   1600 UTC, they approached 13.0 km, later exceeding this height by 2100 UTC. Cloud top

50   heights then dropped relatively quickly after 0000 UTC on the 2nd, and the clouds had fully

51   dissipated from the field-of-view by 0400 UTC. After a brief spell of liquid-phase clouds

52   observed near midday on the 2nd, cirrus would reappear after 1800 UTC, now topped below 11.0

53   km. The period of unusually high-topped cirrus lasted approximately twelve hours, with distinct

54   ascent and descent apparent in cloud structure on either temporal side of the event.

55

56   ***Synoptic and Thermodynamic Environment.***   Shown in Fig. 2 are composite mean 200

57   hPa geopotential height fields (m) and anomalies (shaded) for 1-2 January 2017 derived from the

58   National Center for Environmental Prediction and National Center for Atmospheric Research

59   (NCEP/NCAR) meteorological reanalysis dataset for western North America[2]. Split flow in the

60   midlatitude westerlies beginning in advance of 180° W led into a broad and high amplitude

61   anticyclone centered along 150° W encompassing all of mainland Alaska and most of the

62   Aleutian Islands. Fairbanks was positioned along the northern edge of the largest positive height

63   anomalies, exceeding +400 m. The core of the 200 hPa ridge would stay positioned over the

64   north-central Pacific along 150° W in the Gulf of Alaska. Its axis, however, would shift

65   eastward on 3 January to along and east of the United States/Canada border, pushing even further

66   inland through western Canada on the 4th. Corresponding surface pressures were extremely high

67   as the anticyclone ridge passed over the state, with a 1048 hPa maximum observed over the

---

[2] https://www.esrl.noaa.gov/psd/data/composites/day/

68   Wrangell-St. Elias National Park in the southeast portion of mainland Alaska at 0000 UTC on

69   the 2nd (not shown).

70   The 0000 UTC 2 January 2017 thermodynamic radiosonde profile recorded by the National

71   Weather Service (NWS) office at Fairbanks (Fig. 3) highlights a local tropopause height near

72   13.0 km MSL, measured a few hours after the highest cirrus cloud top heights were observed

73   (Fig. 1). Temperatures are this level were near -75° C (198 K). As suggested earlier, this

74   sounding profile at upper levels was more typical of the sub-tropics and summertime mid-

75   latitudes, aside from the roughly 10° C surface inversion and stagnated cold air mass confined

76   within the local Tanana Valley. The 200 hPa height surface was measured at 11.8 km, or 0.1 km

77   higher than depicted in the reanalysis composite mean (Fig. 2). When considering the spatial

78   and temporal averaging inherent within global reanalysis products, it is likely that the

79   geopotential height anomalies depicted there are relatively low.

80   The influence of the strong anticyclone advancing over the region is further illustrated using

81   virtual potential temperature profiles for all NWS radiosondes launched between 0000 UTC 30

82   December 2016 and 0000 UTC 4 January 2017 (Fig. 4). Constant isentropic surfaces are

83   depicted within the successive profiles in 5 K intervals from 310 - 380 K. Assuming (safely) that

84   the ridge axis passed over the site between 1200 UTC on the 1st and 0000 UTC on the 2nd, rapid

85   isentropic ascent of air can then be seen over the 36-48 hr period beginning 0000 UTC on the

86   31st. This was likely the most significant contributing factor to the deep cirrus clouds observed.

87   As depicted, the upper tropospheric "frontal" boundary separating relatively warm and cold air

88   masses reached as low as 9.5 km on the 31st along the 330 K isentrope, eventually capping out

89   near/above 13.0 km at 0000 UTC on the 2nd. After the axis passed, however, adiabatic

90 subsidence occurred immediately, consistent with cloud dissipation observed near 0400 UTC on

91 the 2nd.

92   The colder and denser air driving the elevated front induced significant uplift; the bulk of

93 which would peak at the tropopause itself at/above 13.0 km. This synoptic uplift no doubt aided

94 in the gradual deposition of water vapor on nascent haze particles, while gravity wave breaking

95 at the tropopause may have caused additional uplift resulting in sufficient atmospheric

96 conditioning for homogenous ice nucleation. This is speculative, however.   The distinct

97 fallstreak nature of the clouds depicted in the lidar imagery suggests rapid crystal growth and

98 relatively large fall speeds. These properties are more traditionally observed from the large ice

99 crystals formed via heterogeneous freezing mechanisms, suggesting homogeneous nucleation

100 was perhaps not the preferred formation mechanism.   Tropopause folding and/or locally-

101 enhanced stratospheric aerosol concentrations acting as ice nuclei were likely not significant

102 factors.

103   These points are reinforced in Fig. 5, which depicts an automated digital image of the cloud

104 scene over Fairbanks late afternoon locally on 1 January (0212 UTC 2 January). Though cirrus

105 clouds remained present over the MPLNET site at UAF, albeit at quickly lowering top heights,

106 only those clouds illuminated along the upper troposphere by the setting sun are distinguishable.

107 These clouds were situated south of Fairbanks nearing the Alaska Range, including Denali

108 National Park (~ 200 km south of the lidar site). The clouds appear reasonably dense, and again

109 could have been confused for lenticular polar stratospheric clouds. Still, fibrous elements are

110 also apparent, which again supports the likelihood of relatively large crystals and enhanced

111 fallstreak presence. Ultimately, though, the point is not necessarily to resolve such nucleation

112 pathways directly, as much as it is recognizing the correlative synoptic ingredients in place to

113   induce and sustain cirrus cloud formation in air advecting along and passing over/through the

114   anticyclonic ridge axis.

115

116   ***Climatological Significance.***   As the MPLNET instrument has only been in place at

117   Fairbanks since October 2016, climatological information on cirrus cloud occurrence is instead

118   taken regionally from the satellite-based NASA Cloud Aerosol Lidar with Orthogonal

119   Polarization (CALIOP). Shown in Fig. 6 are histograms in 1.0 km segments of relative cirrus

120   cloud occurrence measured by Version 3 CALIOP Level 2 Cloud Profile products from 2006-

121   2015 (i.e., total cloud observations at 5-km resolution) over a 5°x5° sector centered on Fairbanks

122   as a function of cloud top height both for December/January and annually. Cirrus were

123   specifically distinguished in the CALIOP datasets as those clouds exhibiting top height

124   temperatures colder than -37° C and warmer than -75° C. The former threshold corresponds

125   with the approximate threshold for the homogeneous freezing of liquid water, which has been

126   shown highly consistent for distinguishing cirrus clouds from autonomous lidar measurements.

127   The latter is chosen conservatively to limit the influence of polar stratospheric clouds possible

128   within the dataset.

129   Annually, a highly limited number of observations have been collected with CALIOP for

130   cirrus cloud top heights exceeding 13.0 km. The bulk of the observations occur with cloud top

131   heights between 8.0 and 10.0 km, consistent with reasonable expectation for such relatively cold

132   latitudes, though a relatively significant number of cases (surprisingly?) do occur above 11.0 and

133   12.0 km. In December/January, the distribution is naturally shifted toward lower heights given

134   the relatively colder endemic airmass regionally. Only a very limited number of observations

135   have been collected at heights above 13.0 km, corresponding with only ten distinct events

136   annually and two during December and January. This implies that the clouds described here are

137   sufficiently rare, though not completely unheard of.

138

139   ***Summary and Perspective.***   Lidar measurements of unusually deep cirrus clouds over

140   Fairbanks, Alaska collected on New Year's Day 2017 are described, with top heights exceeding

141   13.0 km. The synoptic and thermodynamic environment sustaining cloud formation featured an

142   abnormally deep and broad anticyclone with corresponding sharp elevated frontal boundary

143   passing over the central interior of Alaska. Split midlatitude westerly flow over the central

144   Pacific gave way to the large amplitude anticyclone centered over the Gulf of Alaska. The

145   formation of such deep cirrus clouds is considered rare in the wintertime Alaskan sub-Arctic,

146   after comparison with climatological cloud properties derived regionally and seasonally from

147   satellite lidar measurements. The synergy between active-based lidar profiling and operational

148   radiosonde profiling of local thermodynamic properties at Fairbanks helps distinguish the

149   tropospheric nature of the clouds, as compared with polar stratospheric clouds for which they

150   could have been confused for at such heights during the sub-Arctic winter.

151   The remaining point to be made in the case analysis, then, relates to our understanding of

152   how rare this event may or may not prove in the future. Polar meteorology, particularly around

153   the Arctic, is experiencing significant change. Surface temperatures near the North Pole during

154   fall and winter months approaching and exceeding 0° C have been occurring at increasingly

155   alarming rates in recent years. How cirrus clouds respond, however, is an equally compelling

156   question to monitor in coming years compared with such newsworthy instances. Far from being

157   insignificant contributors to climate, changes in basic cirrus cloud macrophysical and occurrence

158   characteristics may in fact prove a bellwether to regional climate change, given their correlative

159 nature relative with local weather processes. The deployment of sufficient ground-based

160 infrastructure is critical to monitoring cirrus, given the indefinite lifetime for CALIOP, the

161 uncertainties surrounding follow-on satellite lidar missions and an inability to resolve all cirrus

162 from radiometric imagers due to their translucent nature.

163

FOR FURTHER READING

Campbell, J. R., D. L. Hlavka, E. J. Welton, C. J. Flynn, D. D. Turner, J. D. Spinhirne, V. S. Scott, and I. H. Hwang, 2002: Full-time, eye-safe cloud and aerosol lidar observation at Atmospheric Radiation Measurement program sites: instruments and data analysis. *J. Atmos. Oceanic Technol., **19,** 431-442.

Campbell, J. R., Vaughan, M. A., Oo, M., Holz, R. E., Lewis, J. R., and Welton, E. J., 2015: Distinguishing cirrus cloud presence in autonomous lidar measurements. *Atmos. Meas. Tech.*, *8,* 435-449, doi:10.5194/amt-8-435-2015.

Campbell, J. R., S. Lolli, J. R. Lewis, Y. Gu, and E. J. Welton, 2016: Daytime cirrus cloud top-of-atmosphere radiative forcing properties at a midlatitude site and their global consequence. *J. Appl. Meteorol. Clim.*, **55,** 1667-1679, DOI:10.1175/JAMC-D-15-0217.1.

Cantrell, W., and A. Heymsfield, 2005. Production of ice in tropospheric clouds: a review. *Bull. Amer. Meteorol. Soc.*, **86,** 795-807.

Lolli, S., J. R. Campbell, J. R. Lewis, Y. Gu, J. W. Marquis, B. N. Chew, S.-C. Liew, S. V. Salinas, and E. J. Welton, 2016: Daytime top-of-the-atmosphere cirrus cloud radiative forcing properties at Singapore. *J. Appl. Meteorol. Clim.*, *in press*.

Mace, G. G., Q. Zhang, M. Vaughan, R. Marchand, G. Stephens, C. Trepte, and D. Winker, 2009: A description of hydrometeor layer occurrence statistics derived from the first year of merged CloudSat and CALIPSO data. *J. Geophys. Res.*, *114*, D00A26, doi:10.1029/2007JD009755.

199   Sassen, K., and J. R. Campbell, 2001: A remote sensing midlatitude cirrus cloud climatology: I.

200   macrophysical and synoptic properties. *J. Atmos. Sci.*, **58,** 481-496.

201   Shupe, M. D., V. P. Walden, E. Eloranta, T. Uttal, J. R. Campbell, S. M. Starkweather, and M.

202   Shiobara, 2011: Clouds at Arctic atmospheric observatories, Part I: occurrence and

203   macrophysical properties. *J. Appl. Meteorol. Clim.*, **50,** 626-644, DOI:

204   10.1175/2010JAMC2467.1.

205   Stubenrauch, C. J., and Coauthors, 2013: Assessment of global cloud datasets from satellites.

206   *Bull. Amer. Meteor. Soc.*, **94,** 1031–1049, doi:10.1175/BAMS-D-12-00117.1.

207   Winker, D. M., and Coauthors, 2010: The CALIPSO mission: a global 3D view of aerosols and

208   clouds. *Bull. Amer. Meteor. Soc.*, **91,** 1211–1229, doi:10.1175/2010BAMS3009.1.

209   **FIGURE CAPTIONS**

210

211   **Figure 1.** NASA Micro Pulse Lidar Network Level 1 normalized relative backscatter

212   (MHz·km^2·uJ^{-1}) measurements collected at Fairbanks, Alaska on 1 January 2017. The

213   MPLNET site at Fairbanks, Alaska is denoted by the blue circle. All heights in km above

214   mean sea level (MSL). Cirrus cloud top heights reaching 13.2 km are depicted by dashed

215   white line.

216

217   **Figure 2.** National Center for Environmental Prediction and National Center for Atmospheric

218   Research (NCEP/NCAR) meteorological reanalysis composite mean 200 hPa

219   geopotential height (m; black contours) and corresponding climatological anomalies for

220   1-2 January 2017 over western North America. The MPLNET site at Fairbanks, Alaska

221   is denoted by the blue circle.

222

223   **Figure 3.** Radiosonde profile of temperature (red) and dewpoint (blue), including wind speed

224   and direction (right side; kts) collected 0000 UTC at Fairbanks, Alaska on 2 January

225   2017.

226

227   **Figure 4.** Upper-tropospheric virtual potential temperature (solid; K) derived from successive

228   radiosonde-based thermodynamic profiles collected at Fairbanks, Alaska every twelve

229   hours between 0000 UTC 31 December 2016 and 0000 UTC 4 January 2017. Isentropes

230   (dashed) are contoured between each profile in 5 K intervals.

231

232   **Figure 5.**   Automated digital photo composite of the late afternoon cloud sky over Fairbanks at

233   0212 UTC 2 January 2017. The camera is oriented toward the south-southwest looking

234   over downtown in the Tanana Valley. The MPLNET site is off to the west of the image.

235   (Photo credit to Todd Thompson of the Fairbanks North Star Borough Air Quality

236   Office).

237

238   **Figure 6.**   Histograms in 1.0 km segments of observations for cirrus cloud top height (km)

239   derived from 2006-2015 CALIOP Level 2 5-km Cloud Profile datasets over a 5°x5°

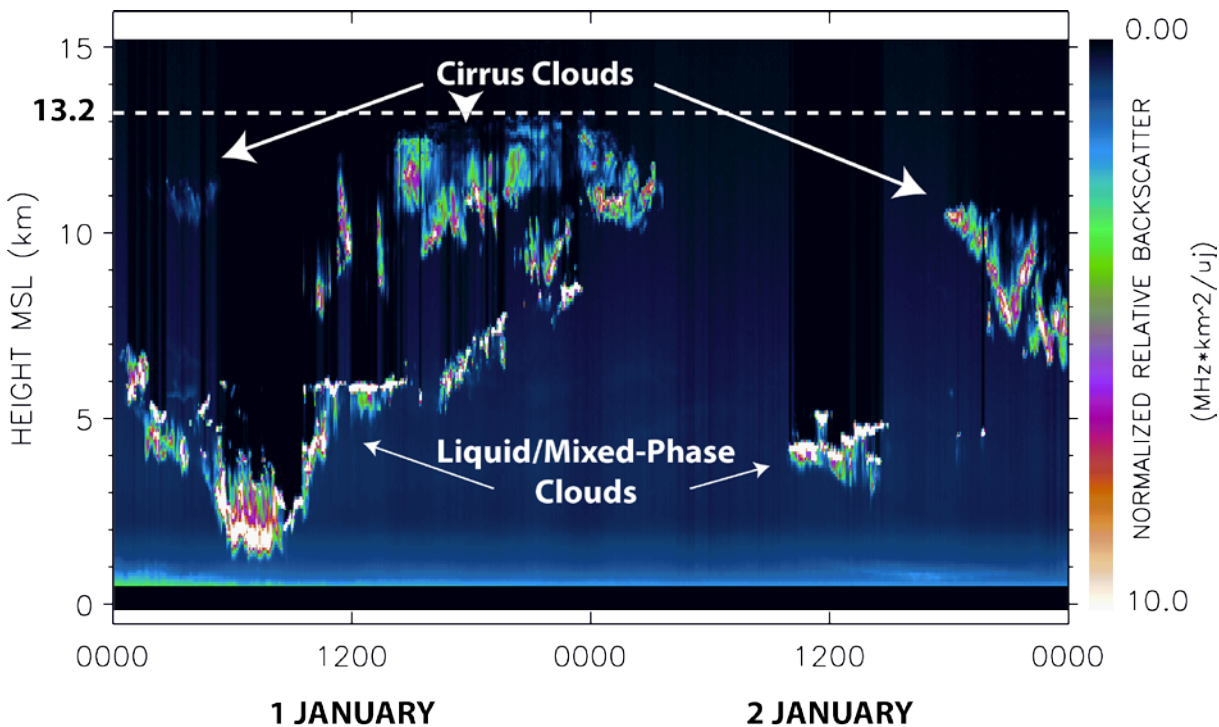240   region centered on Fairbanks, Alaska for (a) December-January and (b) annual.

FIGURE 1

NASA Micro Pulse Lidar Network (MPLNET) Level 1 normalized relative backscatter (MHz·km^2·uJ^{-1}) measurements collected at Fairbanks, Alaska on 1-2 January 2017. All heights in km above mean sea level (MSL). Cirrus cloud top heights reaching 13.2 km are depicted by dashed white line.
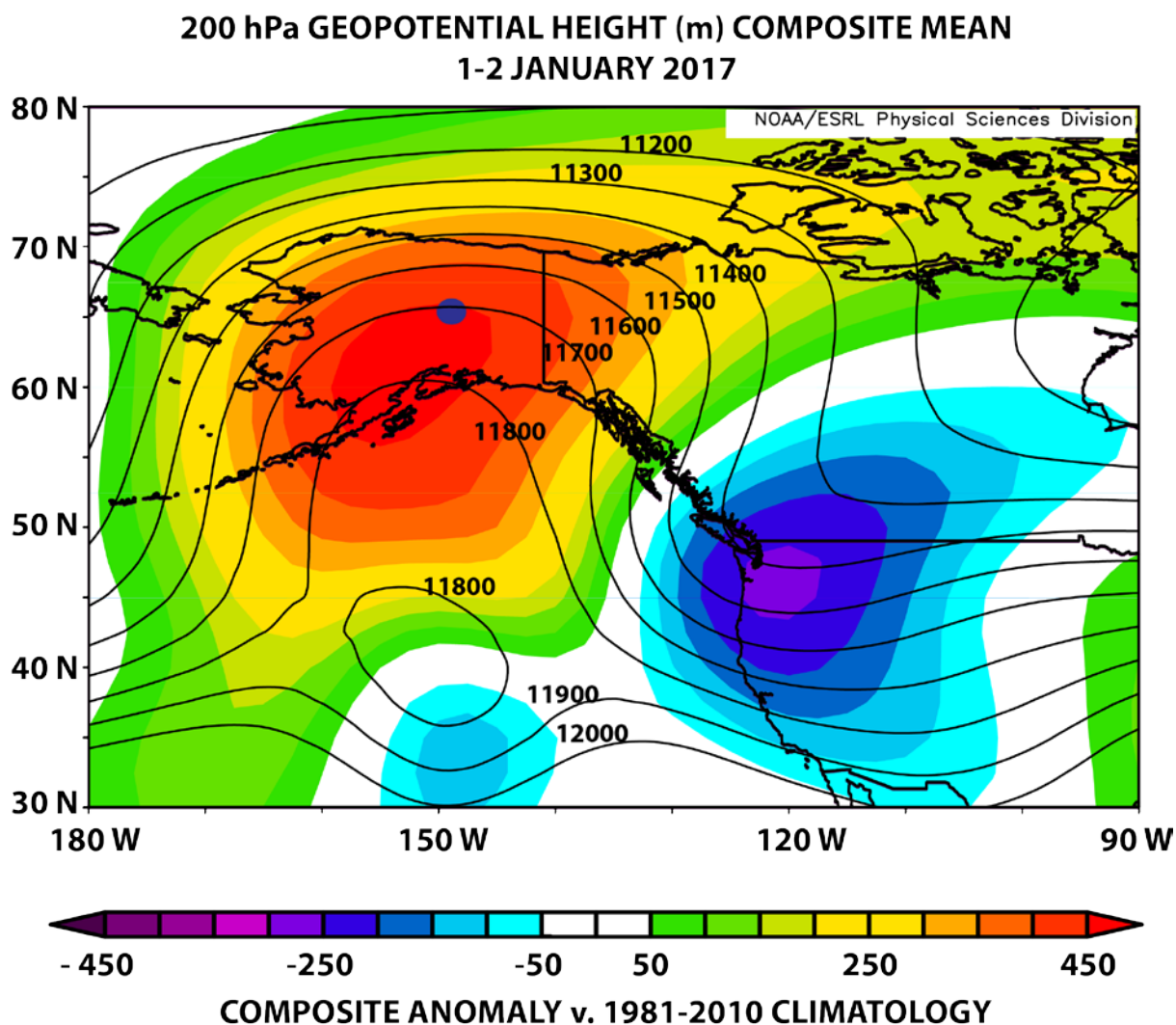
200 hPa GEOPOTENTIAL HEIGHT (m) COMPOSITE MEAN
1-2 JANUARY 2017

FIGURE 2

National Center for Environmental Prediction and National Center for Atmospheric Research (NCEP/NCAR) meteorological reanalysis composite mean 200 hPa geopotential height (m; black contours) and corresponding climatological anomalies for 1-2 January 2017 over western North America. The MPLNET site at Fairbanks, Alaska is denoted by the blue circle.
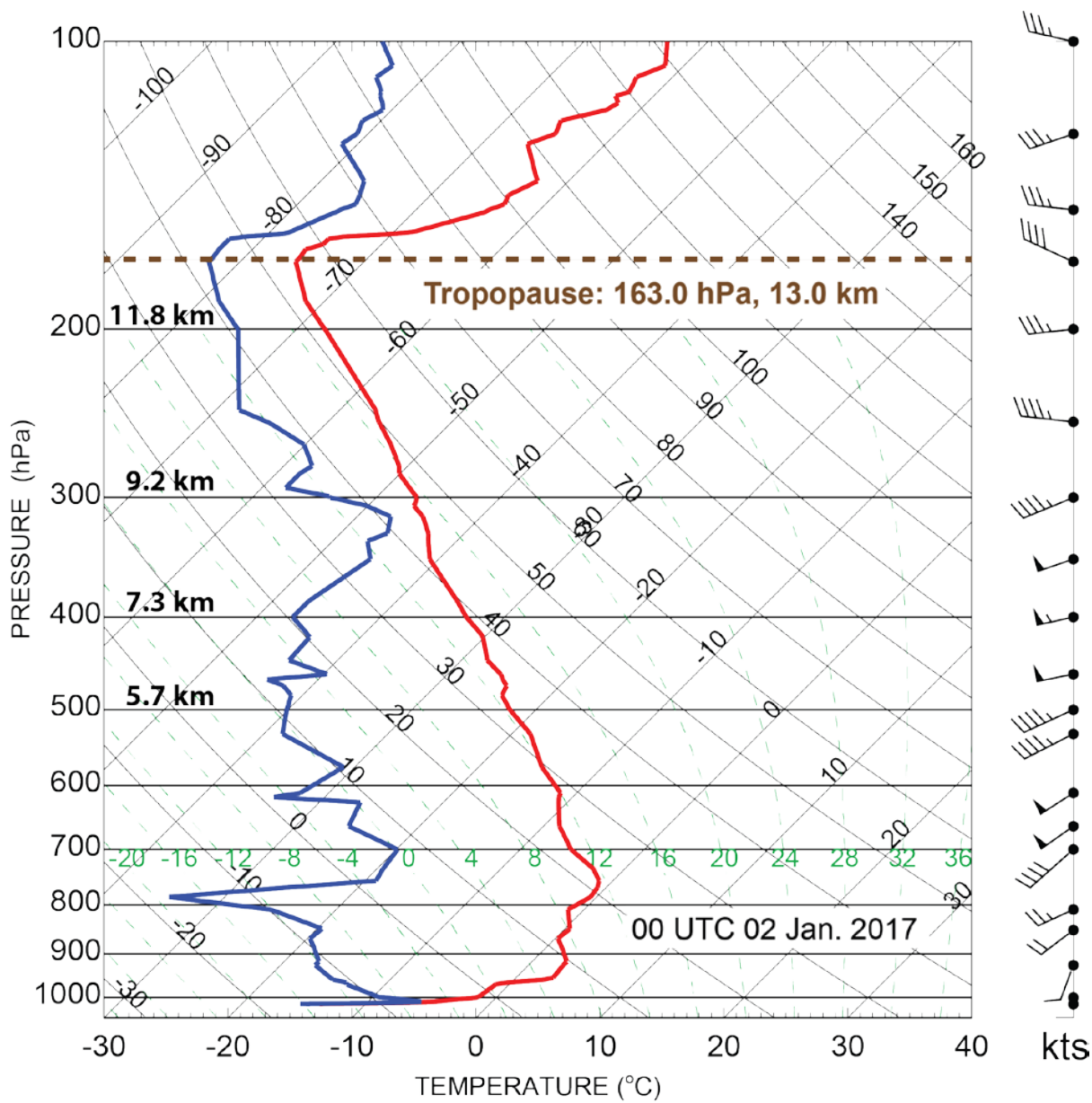
FIGURE 3

Radiosonde profile of temperature (red) and dewpoint (blue), including wind speed and direction (right side; kts) collected 0000 UTC at Fairbanks, Alaska on 2 January 2017.
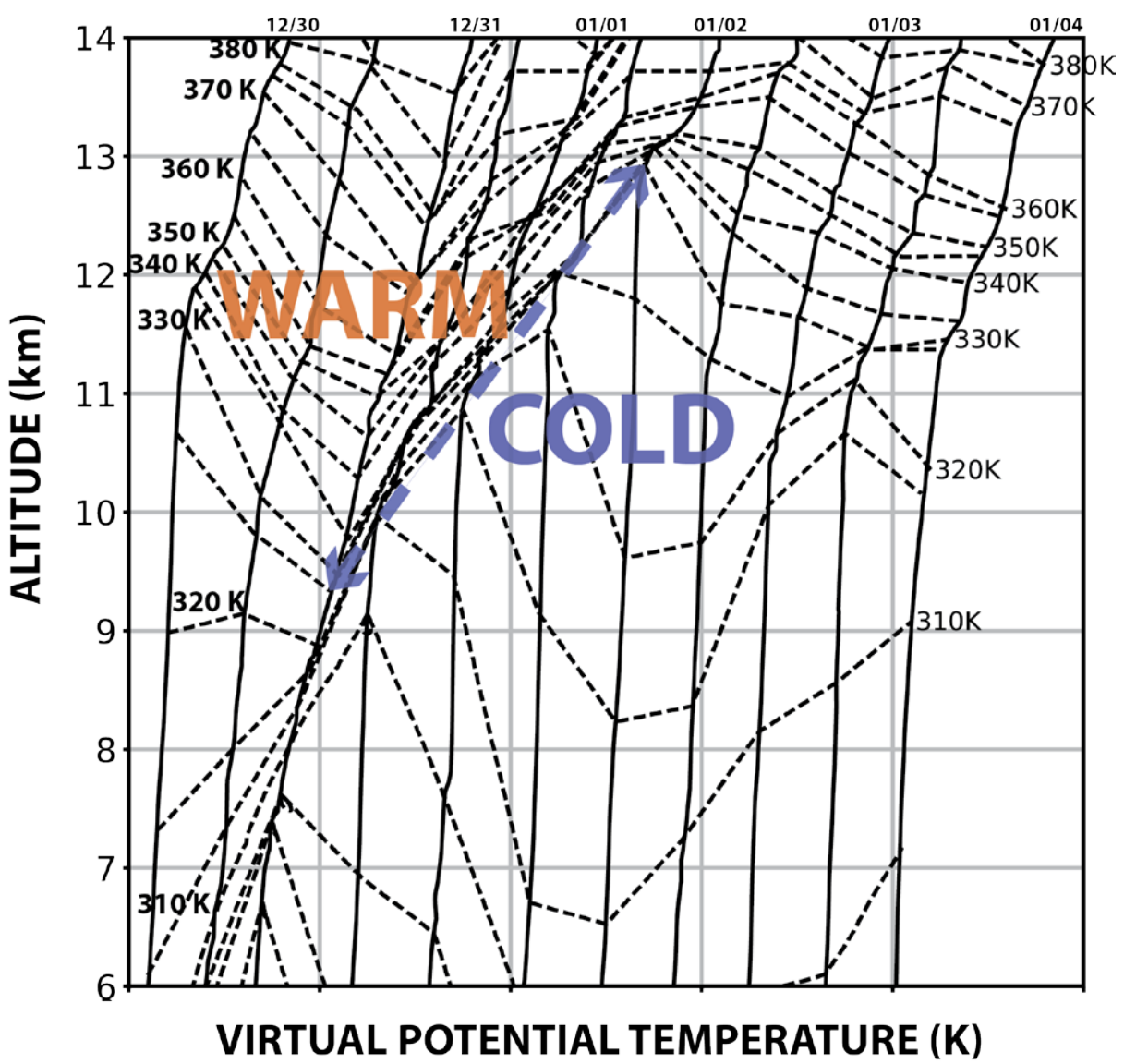
243

FIGURE 4

Upper-tropospheric virtual potential temperature (solid; K) derived from successive radiosonde-based thermodynamic profiles collected at Fairbanks, Alaska every twelve hours between 0000 UTC 31 December 2016 and 0000 UTC 4 January 2017. Isentropes (dashed) are contoured between each profile in 5 K intervals.

244

245

246

FIGURE 5

Automated digital photo composite of the late afternoon cloud sky over Fairbanks at 0212 UTC 2 January 2017. The camera is oriented toward the south-southwest looking over downtown in the Tanana Valley. The MPLNET site is off to the west of the image. (Photo credit to Todd Thompson of the Fairbanks North Star Borough Air Quality Office).
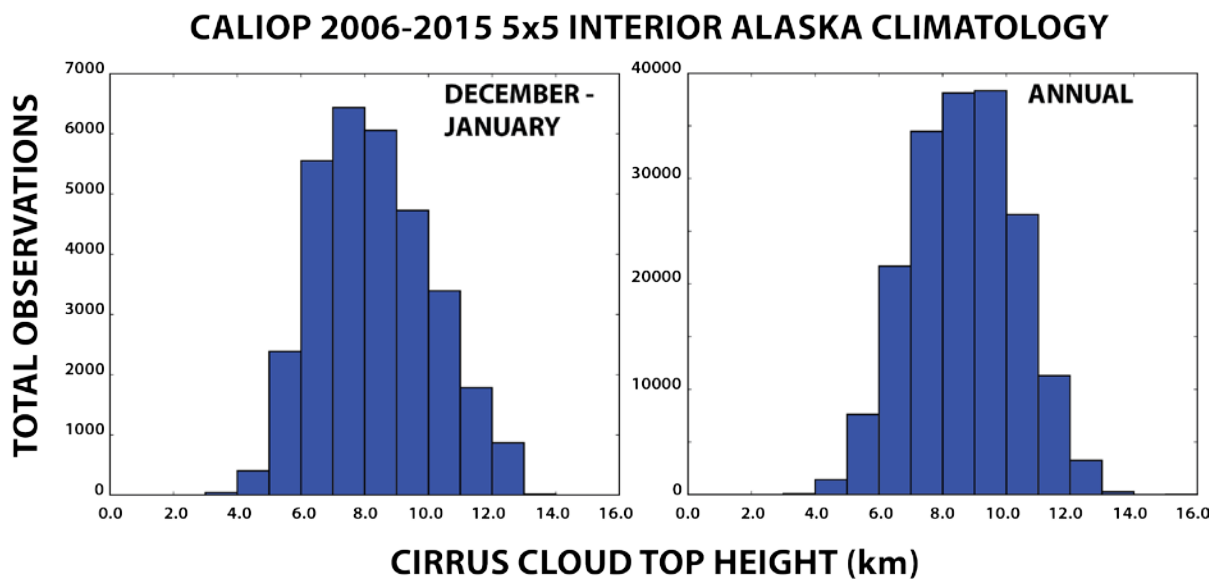
CALIOP 2006-2015 5x5 INTERIOR ALASKA CLIMATOLOGY

FIGURE 6

Histograms in 1.0 km segments of observations for cirrus cloud top height (km) derived from 2006-2015 CALIOP Level 2 5-km Cloud Profile datasets over a 5°x5° region centered on Fairbanks, Alaska for (a) December-January and (b) annual.

247